Article

Biomimetic sheath membrane via electrospinning for anti-adhesion of repaired tendon

Shen Liu, Jingwen Zhao, Hongjiang Ruan, Tingting Tang, Guangwang Liu, Degang Yu, Wenguo Cui, and Cunyi Fan

Biomacromolecules, **Just Accepted Manuscript** • Publication Date (Web): 01 Oct 2012

Biomimetic sheath membrane via electrospinning for anti-adhesion of repaired tendon

Shen Liu[a]‡, Jingwen Zhao[c]‡, Hongjiang Ruan[a], Tingting Tang[d], Guangwang Liu[d], Degang Yu[d], Wenguo Cui[bc], Cunyi Fan[a]

Shen Liu [a] ‡: liushensjtu@sjtu.edu.cn

Jingwen Zhao [c] ‡: smilelooover@sjtu.edu.cn

Hongjiang Ruan [a]: ruanhongjiang@sjtu.edu.cn

Tingting Tang [d]: tingtingtang@hotmail.com

Guangwang Liu [d]: wshlgw@sjtu.edu.cn

Degang Yu [d]: ydg@sjtu.edu.cn

Wenguo Cui [b,c]: wgcui80@hotmail.com

Cunyi Fan [a]: fancunyi888@hotmail.com

[a] Department of Orthopaedics, Shanghai Sixth People's Hospital, Shanghai Jiaotong University School of Medicine, 600 Yishan Road, Shanghai 200233, P.R. China

[b] Orthopedic Institute, Soochow University, 708 Renmin Road, Suzhou, Jiangsu 215007, P.R. China

[c] School of Biomedical Engineering and Med-X Research Institute, Shanghai Jiao Tong University, 1954 Hua Shan Road, Shanghai 200030, P.R. China

[d] Shanghai Key Laboratory of Orthopaedic Implants, Department of Orthopaedics, Shanghai Ninth People's Hospital, Shanghai Jiaotong University Schoole of Medicine, 639 Zhizaoju

Road, Shanghai 200011, P.R. China.

ABSTRACT

The hierarchical architecture and complex biologic functions of native sheath make its biomimetic substitute a daunting challenge. In this study, a biomimetic bi-layer sheath membrane consisting of hyaluronic acid-loaded Poly(ε-caprolactone) (HA/PCL) fibrous membrane as the inner layer and PCL fibrous membrane as the outer layer was fabricated by a combination of sequential and microgel electrospinning technologies. This material was characterized by mechanical testing and analysis of morphology, surface wettability and drug release. Results of an in vitro drug release study showed sustained release. The outer layer had fewer cells proliferating on its surface compared to tissue culture plates or the inner layer. In a chicken model, peritendinous adhesions were reduced and tendon gliding were improved by the application of this sheath membrane. Taken together, our results demonstrate that such a biomimetic bi-layer sheath can release HA sustainably, as well as promoting tendon gliding and preventing adhesion.

KEYWORDS

electrospun fiber; biomimetic; tendon sheath; tendon gliding; adhesion prevention.

I. Introduction

Biomimetic substitutes have been developed to replicate natural tissue for use in the repair of destroyed tissues such as bone[1], articular cartilage[2] and tendon[3] in order to improve functional outcome. The use of tissue-mimicking substitutes potentially provides a promising strategy to restore function or achieve favorable responses for tissue regeneration.[4] To further reduce or to repair damage, biological replication of the tendon sheath is also necessary because it allows the tendon to glide smoothly within it. However, the hierarchical architecture and complex functions of the tendon sheath makes the creation of a substitute a daunting challenge.

The tendon sheath is a membrane-like structure consisting of an outer fibrotic layer and an inner synovial layer. The fibrotic layer prevents exogenous healing of the tendon as an effective biological barrier[5] while the synovial layer secretes synovial fluid mainly containing hyaluronic acid (HA), a crucial source of nutrition for the tendon[6,7] and a lubricant for tendon gliding.[8,9] Tendon sheath-like tissue[10, 11] has been engineered to create a tendon sheath similar to the native one while both HA gel and HA membrane[12-14] have been developed as physical barriers with a lubricant effect. However, the shortcomings of them are that they do not release synovial fluid and that HA has a limited half-life in tissues. Consequently, to fully replicate the functions and structure of the native sheath, it will be necessary to load HA onto some form of biomaterial as a lubricant layer from which it can be released to mimic the function of the inner synovial layer secreting synovial fluid, and to surround this with a barrier layer similar to the outer fibrotic layer of the native sheath.

Biomaterials as barriers have desirable mechanical properties and are easy to handle[15]. Among them, polycaprolactone (PCL) is a widely used biomedical polymer owing to its biodegradability and stability. Thus, PCL has shown preliminary anti-adhesive effects in

reducing intra-abdominal adhesion formation.[16] Specifically, electrospun nanofiber matrices are characterized by a high aspect ratio and a high porosity, and thus are promising materials for drug delivery.[17, 18] Therefore, electrospun PCL may enable the continuous release of the HA. Furthermore, when used as anti-adhesion barriers, the fibrous membranes can allow diffusion of nutrients from outside of the sheath to the covered site, and thus promote intrinsic tendon healing[19]. However, it is difficult to carry out electrospinning of a HA/PCL solution because HA is only soluble in aqueous solution while PCL is soluble in certain organic solvents.

Above all, to replicate the hierarchical architecture and complex biologic functions of a native sheath, a biomimetic sheath should consist structurally of an outer anti-adhesion layer and an inner lubricant layer. Specifically, the inner layer should mimic the biological function of secreting HA to enable tendon gliding. Microgel electrospinning is a new technology for fabricating a composite material based on microgel particles trapped inside nanofibers.[20-22] Jo et al. encapsulated poly(methyl methacrylate) and poly(N-isopropylacrylamide) microgels inside PCL microfibers.[20] Diaz et al. reported on the encapsulation by electrospinning of poly(N-isopropylacrylamide)-based monodisperse microgels within microfibers of crosslinked poly(vinylpyrrolidone) up to concentrations of 40 wt.-% of the microgels.[21] Consequently, in this study, after first solving the problem of microgel electrospinning of HA and PCL, we fabricated a biomimetic bi-layer sheath membrane by sequential electrospinning, producing a sheath membrane consisting of a HA-loaded PCL fibrous membrane as the inner layer and a PCL fibrous membrane as the outer layer to mimic the synovial layer and the fibrotic layer, respectively, of a native sheath. Functionally, controlled release of HA from the inner layer can mimic the biological function of HA secretion, while the outer layer mainly serves as a physical barrier, reducing extrinsic healing. The purpose of this study was to evaluate whether this

biomimetic bi-layer sheath membrane can release HA sustainably, promote tendon gliding and prevent adhesion.

II. Materials and methods

Materials. Polycaprolactone (PCL, Mw = 50 kDa, Mw/Mn = 1.6) was prepared by bulk ring-opening polymerization (Jinan Daigang Co., Jinan, China). Fermentation-derived hyaluronan (HA, sodium salt, Mw = 1.0 MDa) was purchased from Sigma–Aldrich Chemical Co. (St. Louis, MO) and used without further purification. Dulbecco's modified Eagle's medium (DMEM) and fetal bovine serum were supplied by Gibco (Grand Island, NY). All other chemicals and solvents were of reagent grade or better and were purchased from GuoYao Regents Company (Shanghai, China), unless otherwise indicated.

Preparation of the bi-layer electrospun fibrous membrane. In this experiment, three solvents, tetrahydrofuran (THF), water (H_2O) and hexafluoroisopropanol (HFIP), were chosen for the electrospinning mixture solvent. These solvents have a very good miscibility. For electrospinning, 1.0 g HA was completely dissolved in 15.0 g H_2O to form the gel (Figure s1a) while 1.0 g PCL was completely dissolved in 3.0 g tetrahydrofuran to a concentration of 25% (w/w) (Figure s1b). Next, various volumes of HA solution were added to the PCL/THF solution and mixed using a vortex mixer, and then 1 g HFIP was added into the solution and further mixed using a vortex mixer and high-speed stirring to form the electrospun solution with dispersed HA microgel in the PCL solution (Figure s1c). Various HA/PCL blended solutions with different weight ratios from 100:0 (pure PCL), 100:4, 100:8 to 100:12 were prepared for electrospinning (The uniform fiber could not be obtained when the higher content of HA solution volume in electrospun solution.). The electrospinning processes were performed as described previously[23]. Briefly, the electrospinning apparatus was equipped with a high-voltage

statitron (Tianjing High Voltage Power Supply Co., Tianjing, China) with a maximum voltage of 30 kV. The flow rate of the polymer solution was controlled by a precision pump (Zhejiang University Medical Instrument Co., Hangzhou, China) to maintain a steady flow from the capillary outlet. Grounded aluminum foil was used as the collector. A biomimetic bi-layer sheath membrane was first fabricated using PCL fibers as the outer layer by electrospinning PCL solution, followed by the addition of the HA/PCL fibers as the inner layer by electrospinning HA/PCL solution, and thus two layers were prepared using a sequential electrospinning technique. Then, the bi-layer membranes were collected on the surface of a roll of aluminum foil and vacuum dried at room temperature for 24 h. The schematic diagram (**Scheme 1**) below illustrates the creation of the bi-layer biomimetic sheath, and the way it is designed to reproduce the bi-layered structure of the natural tendon sheath.

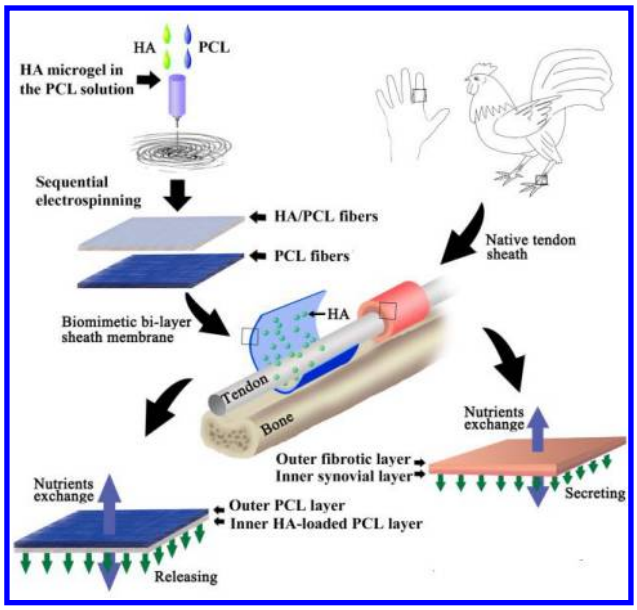

Scheme 1. After formation of HA microgel in the PCL solution, a biomimetic bi-layer sheath membrane was fabricated by sequential electrospinning, producing a sheath membrane consisting ofa PCL-HA fibrous membrane as the inner layer and a PCL fibrous membrane as the outer layer to mimic the synovial layer and the fibrotic layer, respectively, of native sheath.

Characterization of the bi-layer electrospun fibrous membrane. The thickness of the biomimetic bi-layer sheath membrane was measured with a micrometer, and its apparent density and porosity were calculated according to previously published methods[24]. The morphology of the sheath membranes was observed by scanning electron microscopy (SEM, FEI Quanta 200, Netherlands)[25]. Surface wettability of the biomimetic bi-layer sheath membrane was evaluated by the water contact angle (WCA) method at room temperature. The water contact angles of different layers of sheath membranes were measured with a Kruss GmbH DSA 100 Mk 2 goniometer (Hamburg, Germany) followed by image processing of a sessile drop with DSA 1.8 software. For mechanical property tests, the dry biomimetic bi-layer sheath membranes were punched into small strips ($70.0 \times 7.0 \times 0.6$ mm^3). Uniaxial tensile tests were performed using an all purpose mechanical testing machine (Instron 5567, Norwood, MA, 0.5 mm/s, n=5).

In vitro HA release. To evaluate the *in vitro* release behavior of HA, the sheath membranes were first punched into small squares with a total mass of ca. 100 mg, which were immersed in 20 mL of 154 mM phosphate buffered saline (PBS, pH 7.4), containing 0.02% sodium azide as a bacteriostatic agent. The suspension was kept in a constant-temperature shaking water bath (Taichang Medical Apparatus Co., Jiangsu, China) with a shaking speed of 100 cycles/min at a temperature of 37 ℃. At predetermined time intervals, 1.0 ml of the release buffer was removed for analysis and 1.0 ml of fresh PBS was added back for continuing incubation. The samples were stored at 4 ℃ until assayed with a sandwich HA ELISA assay kit (Corgenix, Denver, CO). The assay kit had a detection range between 20 to 800 ng/mL of HA, and some samples were diluted to prevent signal saturation.[26-28]

Cell culture of biomimetic bi-layer sheath membrane. The biocompatibility of the inner

and outer layers was evaluated using multipotent C3H10T½cells (C3) as a cell model. The cells were cultured in DMEM supplemented with 10% fetal bovine serum, 100 U/mL penicillin, and 100 μg/mL streptomycin at 37°C, 5% CO_2 in a humidified incubator. The culture medium was changed every 3 days. After the cells reached 70% confluence, they were harvested with 0.25% trypsin. Discs (diameter, 15 mm) were cut out of the sheath membrane using a punch and placed in the 24-well plate. The samples were sterilized by immersion in 75% ethanol for 1 h and then washed repeatedly with PBS to remove residual ethanol. To seed cells onto the samples, cells were pipetted directly onto the specimens at a density of 2×10^4 cells/cm^2 (for proliferation and morphology assay) or 4×10^4 cells/cm^2 (for live/dead assay) and incubated in complete culture medium for different lengths of time.

Cell proliferation assay. Cells cultured on different specimens were analyzed for proliferation on days 1 and 4 by cell counting. The cells were detached from the surfaces of each specimen by trypsinization and counted with a Beckman Vi-Cell XR Cell Viability Analyzer (Beckman Coulter, Inc., California, American). The results are expressed as the average number of cells attached per cm^2 of surface. The number of cells adhering and growing on different specimens was also observed by scanning electron microscopy (SEM, FEI Quanta 200, Netherlands) after fixation with 2.5% glutaraldehyde (Gibco Laboratories) and following dehydration through a graded ethanol series.

Cell morphology assay by confocal laser scanning microscopy. The cytoskeletal arrangements on sheath membranes and tissue culture plate surfaces were determined by actin staining after 24 h. Briefly, matrices with cells were washed twice in PBS and then fixed in 4% paraformaldehyde for 10 min. After removing the fixative, cells were washed repeatedly in PBS and permeabilized with 0.1% Triton X-100 (Sigma Aldrich) for 10 min. Then, samples with

cells were washed twice in PBS and stained with 20 μg/mL of phalloidin (Sigma) according to the manufacturer's instructions. Finally, cells were washed twice in PBS and stained with 1 μg/mL DAPI for 5 min before imaging under a confocal laser scanning microscope (Leica TCS SP2; Leica Microsystems, Heidelberg, Germany). Results are expressed as the average cell area on different surfaces.

In vitro viability assay. Live/dead staining was used to determine the viability of cells on different surfaces. Viability of cells was evaluated using a Live/Dead stain kit (Invitrogen; Eugene, OR). Cells were seeded onto the samples at a concentration of 4×10^4 cells/cm^2 in a 24-well plate. After culture for 24 h, cells were washed twice in PBS and stained with 2 μM calcein AM and 10 μM EthD-1. Stained cells were observed under a fluorescence microscope (LEICA DM 4000 B). The calcein AM produced an intense uniform green fluorescence in live cells, while EthD-1 produced a bright red fluorescence in dead cells.

Preliminary animal study. All procedures and handling of the animals were carried out in accordance with the policies of Shanghai Jiao Tong University School of Medicine and the National Institutes of Health. Leghorn chickens (1.5–2 kg each) were used for this study. They were anesthetized by intramuscular injection of ketamine hydrochloride (50 mg/kg). Then, sterile skin preparation and an elastic tourniquet were applied. A lateral skin incision was created on the proximal phalanx of the third toe. After incising the flexor tendon sheath, the flexor digitorum profundus (FDP) was isolated, transversely incised and then repaired using a modified Kessler tendon repair with 6-0 prolene suture (Ethicon Ltd., Edinburgh, UK). The animals were randomly assigned to three groups. In groups I and II, a 1 × 1-cm piece of PCL fibrous membrane (PCL-HA 0% sheath membrane) or a sheath membrane loaded with 12% HA was wrapped around the repair site of the FDP, while no treatment was performed before

wound closure in the control group. After skin closure, the extremity was immobilized in a weight-bearing splint.

In vivo macroscopic evaluation. Before sacrificing the animals, the repair site was visually examined for signs of inflammation or ulceration. The severity of peritendinous adhesion was evaluated by a scoring system.[29,30] To evaluate the severity of peritendinous adhesions, an adhesion scoring system was used to grade a particular area into grades 1–5 based on the surgical findings: grade 1, no adhesion; grade 2, adhesion area can be separated by blunt dissection alone; grade 3, adhesion area less than or equal to 50% which required sharp dissection for separation; grade 4, 51–97.5% adhesion area which required sharp dissection for separation; and grade 5, more than 97.5% of the adhesion area requiring sharp dissection for separation.

In vivo histological evaluation. The third toes were fixed in 4% paraformaldehyde for one day and then decalcified in 10% EDTA for 1 month at room temperature. Samples were dehydrated through increasing concentrations of ethanol and then paraffin embedded. Sections were cut in 4-μm sagittal slices and stained with Masson's trichrome. Histologic assessments of adhesions and tendon healing were performed[31,32]. Adhesions were quantified into four grades as follows: grade 4, severe (>66% of the tendon surface); grade 3, moderate (33–66% of the tendon surface); grade 2, mild (<33% of the tendon surface); or grade 1, no adhesions. Tendon healing was quantified into four grades as follows: grade 4, poor (failed healing or massive overgrowth of granulation tissue); grade 3, fair (irregularly arranged and partly broken intratendinous collagen bundles); grade 2, good (intratendinous collagen bundles exhibited good repair, but the epitenon was interrupted by adhesions); or grade 1, excellent (good tendon continuity and smooth epitenon surface). These histological sections were evaluated under light

microscopy (LEICA DM 4000 B) by two independent investigators blinded to the treatment.

In vivo biomechanical evaluation. To evaluate peritendinous adhesions and tendon healing, the work of flexion and the breaking force were both measured using a rheometer (Instron 5548, Instron, Norwood, MA). To evaluate the work of flexion, the proximal end of the FDP tendon was fixed to a force gauge and the proximal phalanx of the toe was attached to a home-made device with the proximal interdigital joint fixed by stainless steel rods. The load (Newtons) and the displacement (mm) were measured when the FDP tendon was pulled at 20 mm/min until the angle of the distal interdigital joint was 40 °. The work of flexion was then calculated by curve integration. To avoid individual variation, both the repaired and the intact tendons of both sides in each animal were evaluated and the ratio of repaired work of flexion vs intact work of flexion was used as a parameter to determine the difference among different groups. To evaluate breaking force, the repaired chicken FDP tendons were harvested. The proximal and distal ends of the tendon were fixed to the force gauge of the rheometer. The tendon ends were pulled apart at a speed of 20 mm/min until rupture of the tendon occurred, and breaking force was recorded by the rheometer.

Statistical analysis. Results are expressed as mean ± standard deviation(SD). Statistical software SPSS 10.0 (Chicago, IL) was used to analyze the data by one-way analysis of variance; $P < 0.05$ was considered significant.

III. Results

Characterization of the biomimetic bi-layer sheath membrane. The cross-sectional and surface fibrous morphology of the biomimetic bi-layer sheath membrane are shown in Figure 1. Results of cross-sectional SEM observations show that the thicknesses of the sheath membranes were near 150 μm for the inner HA-loaded PCL layer and near 80 μm for the outer PCL layer.

It can be seen that there are no beads in the fibrous structure and the fibers are uniform in size, forming randomly interconnected structures and seemingly smooth in all samples. Fiber diameter was 3.66 ± 0.57 μm for the outer PCL layer, while the inner PCL layer with different HA compositions of 0% (PCL-HA0%), 4% (PCL-HA4%), 8% (PCL-HA8%) and 12% (PCL-HA12%), were 3.89 ± 0.59, 3.42 ± 0.62, 2.99 ± 0.54 and 2.86 ± 0.71 μm, respectively. To clarify the effects of the HA on the surface properties of electrospun fibers, water contact angles of electrospun fibrous membranes were measured. The water contact angles were 129.5 ± 2.4, 51.3 ± 4.7, 0 and 0 ° for PCL-HA0%, PCL-HA4%, PCL-HA8% and PCL-HA12%, respectively.

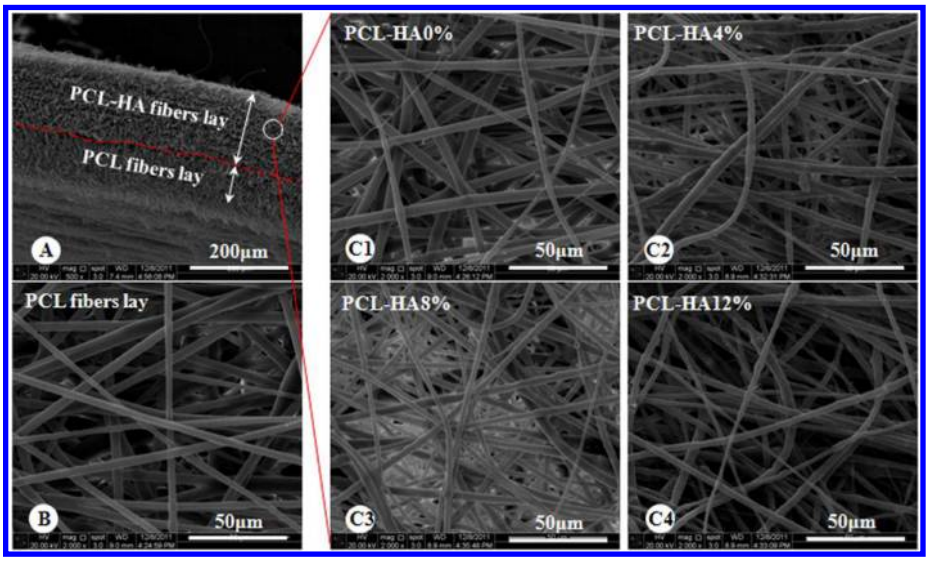

Figure 1. SEM observations showing cross-sectional and surface morphological features of PCL fibers and HA/PCL fibers with different sheath membranes thicknesses. (a) Cross-section of the biomimetic bi-layer sheath membrane. (b) PCL electrospun fibers of the outer layer. (c) PCL-HA0% (c1), PCL-HA4% (c2), PCL-HA8% (c3) and PCL-A12% (c4) electrospun fibers of the inner layer.

Mechanical properties of sheath membranes. To clarify the effects of HA content on the mechanical properties of sheath membranes, stress-strain measurements were conducted and the results are shown in Figure 2. The tensile strengths of the bi-layer of PCL-HA0%, PCL-

HA4%, PCL-HA8% and PCL-HA12% fiber membranes were 2.13 ± 0.25, 1.91 ± 0.21, 1.77 ± 0.18 and 1.55 ± 0.21 MPa, respectively, while the tensile modulus was 19.82 ± 3.33, 23.58 ± 3.66, 26.35 ± 3.70 and 30.13 ± 3.99 MPa, respectively. The tensile strength of the PCL membrane is significantly larger than most of these bi-layer membranes. Although the statistical analysis indicated no significant difference between the bi-layer PCL-HA8% and 12% membranes ($P > 0.05$), the tensile strength and tensile modulus of the bi-layer PCL-HA12% fiber membrane was significantly different from those of the single-layer PCL-HA12% fiber membrane (Table s1). The increase of the tensile modulus reflects the changes of fibers in the membrane from elastic fracture to brittle fracture because of the addition of HA.

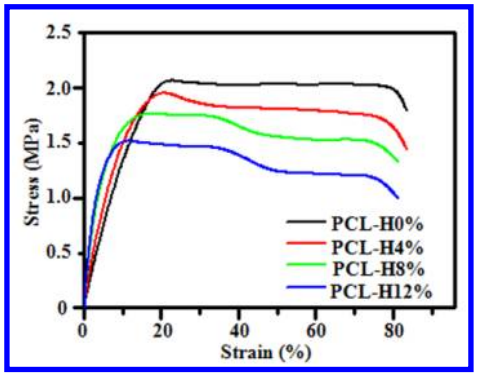

Figure 2. Stress/strain curves for the inner PCL-HA0% (A), PCL-HA4% (B), PCL-HA8% (C) and PCL-HA12% (D) layers.

***In vitro* HA release.** For PCL-HA electrospun fibers, after incubation into the releasing medium, the PCL-HA electrospun fibers gradually infiltrate into the solution. The mixture of PCL-HA fibers starts thickening quickly and becomes a gel around the fibers because of the release of HA. The outer HA gel layer then gradually dissolves into the releasing medium during a high-speed shaking process. It is noted that the HA released from PCL-HA goes through a process, from swelling of the gel to dissolving into water. The release kinetics of HA can be illustrated as a one stage burst release, as shown in Figure 3 A. The release profiles of all

PCL-HA fibers were characterized by a typical biphasic pattern. In the initial phase, a pronounced burst release or steady release phase was observed, and then it tended to plateau or a gradual release followed during the rest period. The total amounts released were 65.8, 79.6 and 88.6% during this stage for PCL-HA4%, PCL-HA8% and PCL-HA12% during the first 96 h, respectively. After the burst release, a residual release of HA was observed for PCL-HA8% and PCL-HA12% electrospun fibers, representing further release of HA from the inner fibers. However, less release from PCL electrospun fibers with 4% HA loading was detected, with an initial burst release of 65.8% followed by sustained release of an additional 35% over 10 days. This indicated the advantages of electrospun fibrous scaffolds with lower HA entrapment in enhancing the slow release of HA. The cumulative quantity of HA released *in vitro* from 100 mg of PCL electrospun fibers with HA loadings of PCL-HA4%, PCL-HA8% and PCL-HA12% is summarized in Figure 3 B. The release profiles of all the fibers were the same up to the cumulative percentage of fast release. Approximately 397, 798 and 1191 μg HA was released in the 14 days as seen in the sheath for PCL-HA4%, PCL-HA8% and PCL-HA12%, respectively. The cumulative quantity of HA could be calculated from the different amounts of electrospun fibers in the scaffold, and this data could be used as reference data for animal testing.

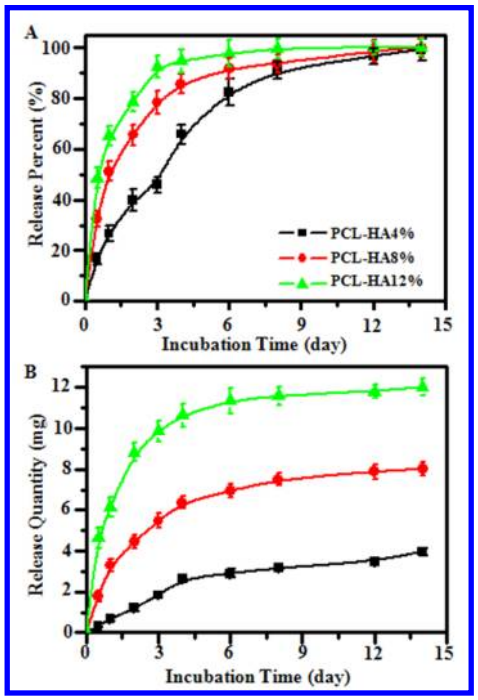

Figure 3. In vitro HA release cumulative percentage (A) and cumulative quantity (B) from electrospun fibers with drug loadings of 4%, 8% and 12% after incubating in PBS at 37 ℃.

***In vitro* cell adhesion and proliferation.** The adhesion and proliferation of C3H10T½ cells on the surface of the tissue culture plate, and on the outer PCL layer and the inner HA-loaded PCL layer of sheath membranes was compared after 1 and 4 days (Figure 4). It was observed that many cells adhered to and proliferated well on the surface of the inner layers, while fewer cells were found to adhere to the surface of the outer PCL layer. The cell adhesion and proliferation on the surfaces of the inner layers increased with increasing HA composition (Figure s2). The number of cells on different surfaces was compared after 1 and 4 days of culture; cell growth on the different surfaces after 4 days showed a similar trend to cell adhesion after 1 day, and cells grew better on the surfaces of the inner layer as the composition of HA increased than on the outer layer after 4 days, but grew best on the control surface of the tissue culture plate (Figure 4 F). The efficiency that trypsinisation can remove cells from fibrous membranes has been verified (Figure s2).

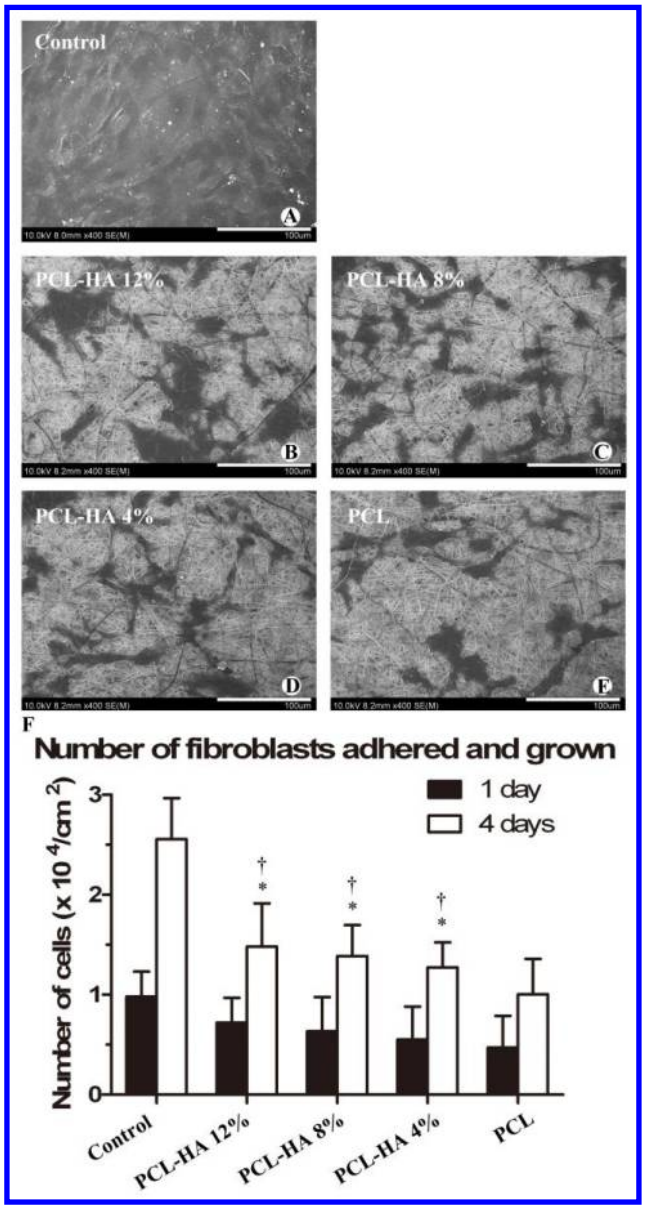

Figure 4. SEM observation of cells growing on the surface of control (A), PCL-HA12% (B), PCL-HA8% (C), PCL-HA4% (D) and PCL (E) sheath membranes on day 4. Cell counts (F) on control, PCL-HA12%, PCL-HA8%, PCL-HA4% and PCL at day 1 and day 4. *P < 0.05 compared with control; †P < 0.05 compared with cells grown on the PCL fibrous membrane. Data are expressed as mean ± SD (each group, n = 3).

In vitro cell morphology. The cytoskeletal arrangement of cells was investigated by

double fluorescence staining with the F-actin protein labeled in red and the nucleus in blue. Based on the images, average cell area on each surface is calculated using Photoshop 8.0 according to the scale bar. By comparing the cell areas on different surfaces, the morphology of cells can be inferred. As shown in Figure 5, cells cultured on the surface of a tissue culture plate as the control had the largest cell area. In addition, the cells developed a flattened morphology on the inner HA-loaded PCL layer with a concentration-dependent effect. Furthermore, the cell areas on the surface of the outer PCL layer were significantly lower than those of the rest of the samples, indicating that the outer PCL layer prevents cell adhesion. These data are in agreement with the images in Figure 5.

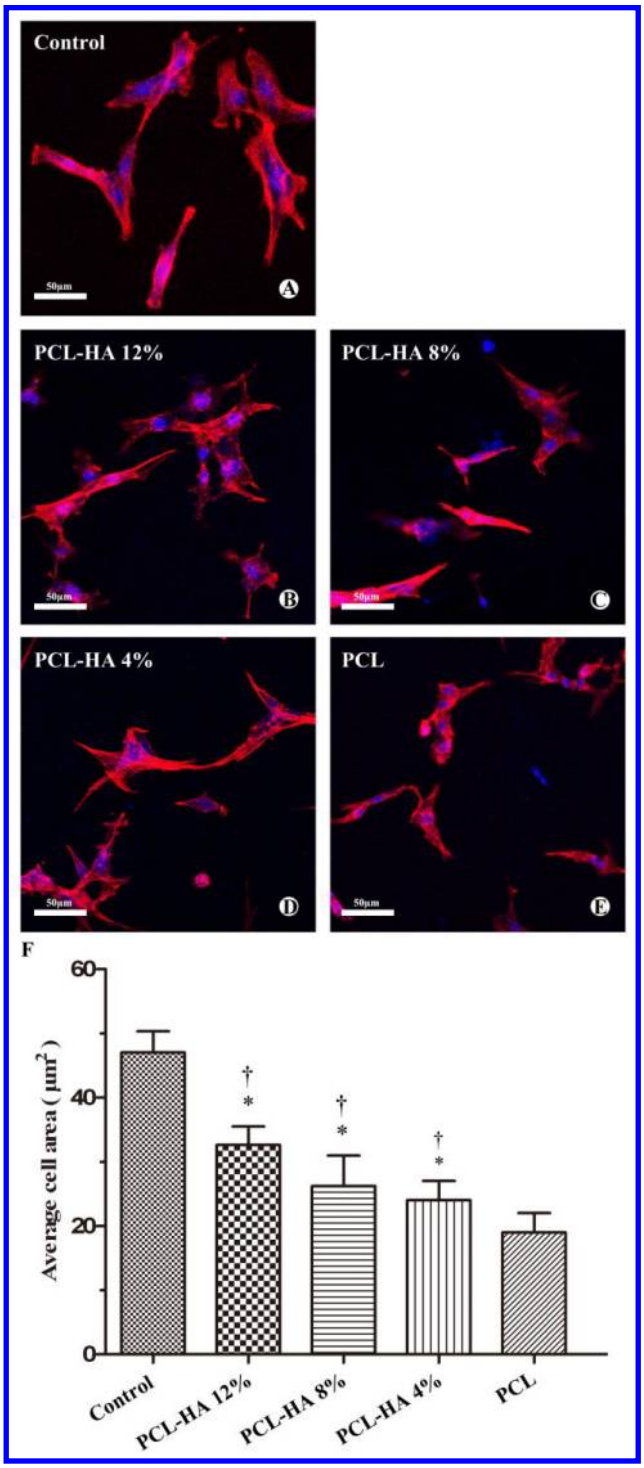

Figure 5. Cytoskeletal arrangement of cells on the surface of control (A), inner PCL-HA12% (B), PCL-HA8% (C) and PCL-HA4% (D) layer and outer PCL layer (E) of sheath membranes. The average cell area was measured and is shown graphically (F). *P < 0.05 compared with

control; †P < 0.05 compared with the group grown on the PCL fibrous membrane. Data are expressed as mean ± SD (each group, n = 3).

Cell viability. Calcein AM should clearly show a uniform green fluorescence in live cells, while EthD-1 produces a bright red fluorescence in dead cells. The cells had grown on all surfaces, but grew less on the surface of the PCL fiber membranes. It was also observed that more cells adhered to and were better distributed on the surface of the inner HA-loaded PCL layer and the tissue culture plate surfaces compared to the outer PCL layer (Figure 6 A-E). Furthermore, the number of dead cells on different surfaces showed the opposite trend to the total number of cells on the same surfaces. Figure 6 F compares the dead/live cell rate adhering to the different surfaces after 1 day of culture.

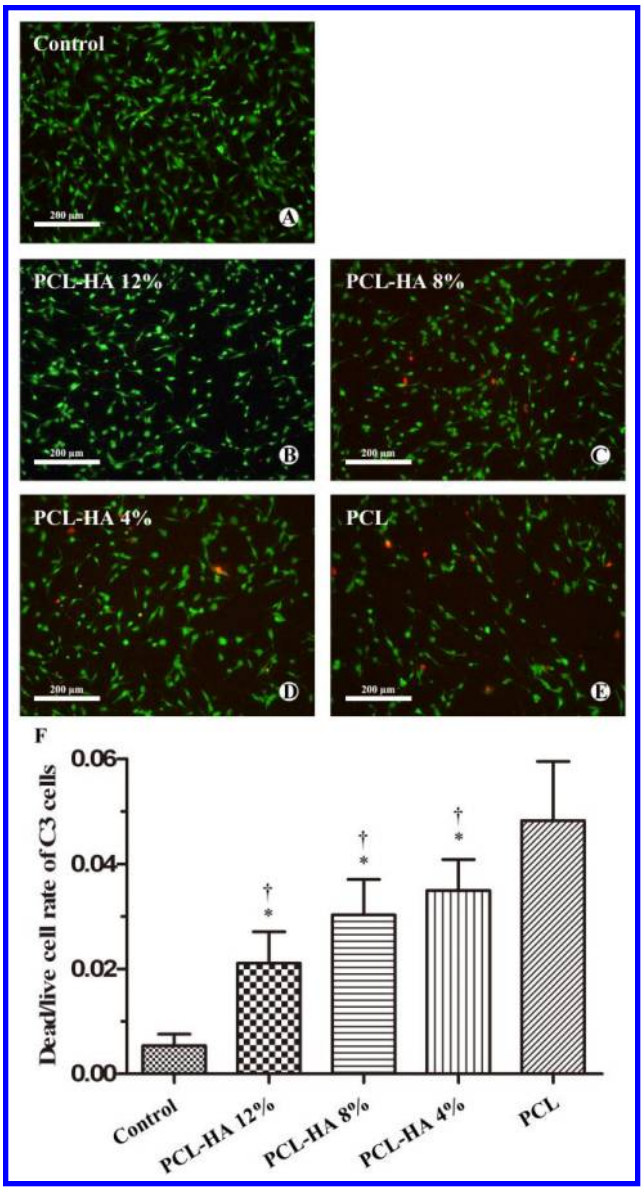

Figure 6. The results of a viability assay of C3H10T½ cells (C3) grown on the surface of control (A), inner PCL-HA12% (B), PCL-HA8% (C) and PCL-HA4% (D) layer and outer PCL layer (E) of sheath membranes. Dead/live rate of cells was counted (F). *P < 0.05 compared with control; †P < 0.05 compared with the group treated with PCL fibrous membrane. Data are expressed as mean ± SD (each group, n = 3).

In vivo gross observation. After 21 days, the peritendinous adhesions were evaluated by

direct observation after surgical exploration of the repair sites (Figure 7). In the untreated control group, large and severe peritendinous adhesion areas were observed at the repair site and required sharp dissection to separate (Figure 7 A). In PCL fibrous membrane treatments (Figure 7 B), although the adhesion area could be separated by blunt dissection, loose bundles of fibrous tissue could be detected. In the tendons treated with biomimetic bi-layer sheath membrane, no formation of adhesions was observed between the repaired tendons and the peritendinous tissues (Figure 7 C). Even if some areas of adhesion could be found, they could easily be separated by blunt dissection. Furthermore, the surfaces of the repaired sites on the tendon were smooth. According to the severity of peritendinous adhesion scores from macroscopic observations, the average scores in the biomimetic bi-layer sheath membrane group were lower than the other groups ($P < 0.05$) (Figure 7 D).

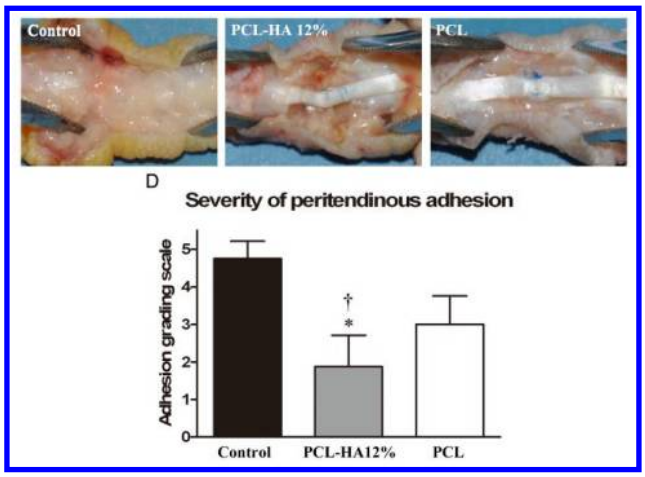

Figure 7. Gross evaluation of a chicken model of flexor digitorum profundus tendon repair after 21 days. (A) Untreated control group; (B) group treated with sheath membrane with inner PCL-HA PCL layer; (C) group treated with PCL membrane. The adhesion was graded according to severity (D) of peritendinous adhesion. *P < 0.05 compared with control; †P < 0.05 compared with the group treated with PCL fibrous membrane. Data are expressed as mean ± SD for 8 tendons/group.

In vivo histological assessments. Histological assessments of the tendons repaired using each of the treatments are shown in Figure 8. The repair sites of untreated tendons were filled with fibrous tissue bridging between the peritendinous tissues and the tendon. Furthermore, obliteration of the tendon sheath space was observed (Figure 8 A). No peritendinous adhesion tissue formation in the group wrapped with biomimetic bi-layer sheath membrane and the tendon sheath space was clear (Figure 8 B). In the tendons wrapped with PCL fibrous membrane, loose bundles of fibrous tissue invaded the partial epitenon layers of the repaired tendons at the two tissue boundaries between the peritendinous tissues and the tendon (Figure 8 C). In addition, intratendinous collagen bundles exhibited better tendon healing when compared with the other two groups. The average scores of adhesions and tendon healing in the biomimetic bi-layer sheath membrane group were lower than the other groups ($P < 0.05$) (Figure 9 D).

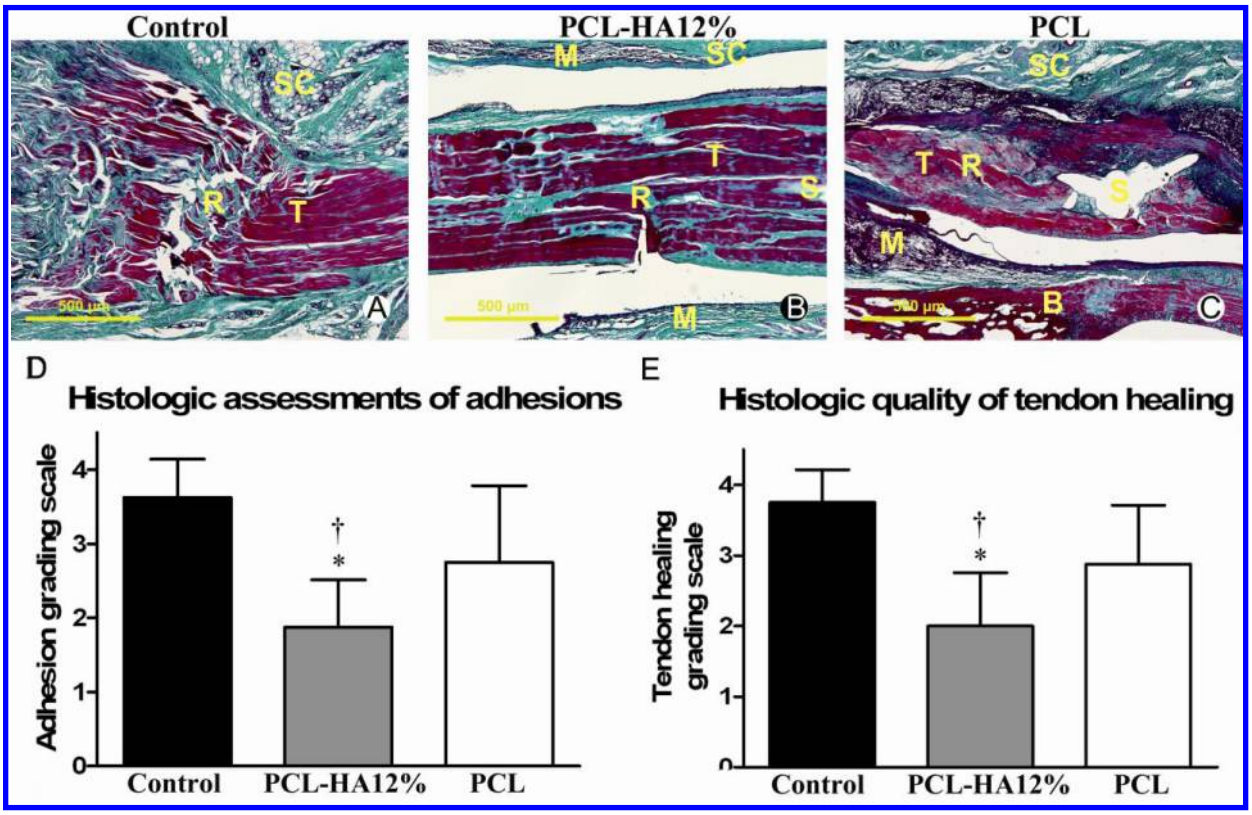

Figure 8. Masson's trichrome staining of untreated repair site (A); repair site wrapped with sheath membrane with inner PCL-HA PCL layer (B); repair site wrapped with PCL membrane (C). Subcutaneous tissue (SC), tendon (T), sutured site (S), bone (B) and materials (M) could be detected. The repaired flexor digitorum profundus tendon was evaluated 21 days after surgery by histologic evaluation of tendon adhesions (D) and histologic quality of tendon healing (E). *P < 0.05 compared with untreated control; †P < 0.05 compared with the group treated with PCL membrane. Data are expressed as mean ± SD for 8 tendons/group.

In vivo biomechanical analysis. Mechanical analyses using a rheometer showed that the ratio of work of flexion representing peritendinous adhesions was significantly lower in the PCL fibrous membrane group than in the control group ($P < 0.05$) (Figure 9 A) while it was significantly lower still in the biomimetic bi-layer sheath membrane group than in the PCL fibrous membrane group. An increase in breaking force could be detected in the sheath membrane group in comparison with the PCL fibrous membrane group, although the breaking force in the group treated with different membranes was still lower than control. However, the breaking force representing tendon healing was not significantly different between the three groups (Figure 9 B).

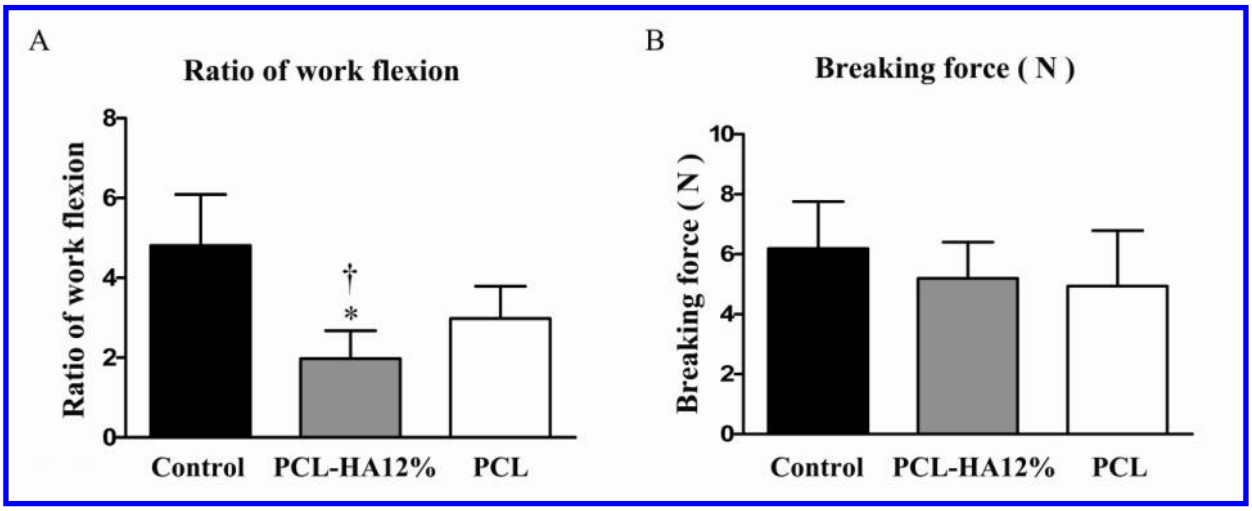

Figure 9. Tendon repair and peritendinous adhesions were evaluated by determining the ratio of work of flexion (A) and the breaking force (B) of the repaired tendons. *P < 0.05 compared with control; †P < 0.05 compared with the group treated with PCL fibrous membrane. Data are expressed as mean ± SD for 8 tendons/group.

IV. Discussion

This report describes the results of a pilot test of the effects of a biomimetic bi-layer sheath membrane to replace the native sheath. HA and PCL were first mixed using the microgel electrospinning technique. An outer PCL layer of the biomimetic sheath was then prepared, then the inner HA-loaded PCL layer was sequentially electrospun onto the PCL layer. Using this method enabled us to create a biomimetic sheath with appropriate flexibility combined with the controlled release of HA. Thus cell adherence and proliferation can be promoted by the release of HA from the inner layer while adhesion is prevented by the outer PCL layer. As shown by our *in vivo* results, adhesion to surrounding tissue was blocked by the outer sheath membrane while the inner HA-loaded PCL layer released HA, promoting tendon gliding.

As shown by SEM (Figure 1 A), such a sheath membrane has a structure mimicking the bi-layer structure of native tendon sheath, which consists of an outer fibrotic layer and an inner synovial layer. Although large numbers of anti-adhesion membranes have previously been applied as physical barriers[33, 34], our novel biomimetic sheath membrane has one significant structural advantage in that the inner layer has unique properties which can satisfy the special needs of tendon healing and gliding. Another structural advantage is that the bi-layer structure solves the problem posed by the addition of HA to PCL, which reduces the anti-adhesion effect of a PCL fibrous membrane, thus enabling the adhesion and proliferation of cells (Figure 4) without impairing the desirable anti-adhesion effect of the PCL in the way that would occur if a

single-layer PCL fibrous membrane combined with HA was applied. Furthermore, although the tensile strength of the bi-layer sheath membranes decreases with increasing HA (Figure 2), the tensile strength of the single-layer 12% HA-loaded PCL fibrous membrane was only 1.26 ± 0.20 MPa(Table s1). It is harder for our surgeons to wrap the single-layer 12% HA-loaded PCL fibrous membrane around the repair site of the FDP. Thereafter, using our bi-layer system, the bi-layer sheath membranes would be expected to have better tensile strength than single layer fibrous membranes. Because of these advantages of the bi-layer sheath membrane, the single-layer PCL/HA membrane was not further applied in the in vivo study.

The main aim of creating an artificial sheath is to achieve better biological function. In previous studies, both HA gel and HA membrane were used in an attempt to reduce tendon adhesion and simultaneously to reduce tendon gliding resistance[12-14]. However, none of the anti-adhesive HA derivative agents were entirely ideal, because their high rheological behavior and rapid degradation limited their clinical uses in hand surgery. Furthermore, in an attempt to create a tendon sheath similar to the native one, Ozturk *et al.*[10] and Liang *et al.* [11] seeded tendon sheath-derived cells onto different biomaterials to engineer HA-producing sheaths. However, although HA was detected in both engineered sheaths, it seems that these single layer sheaths acted mainly as an anti-adhesion barrier, because it was not possible to detect synovial fluid directly released from them. Additionally, seeding cells onto these scaffolds to produce HA-secreting sheaths also has limited therapeutic potential because the supply of seed cells is limited and donor site defects in healthy compartments have to be considered as a potential source of new clinical symptoms. In this study, a biomimetic bi-layer sheath membrane was

developed to provide improved biological function. The outer PCL layer was prepared to recreate the anti-adhesive role of the outer fibrotic layer, preventing tendon adhesion to the surrounding repaired tissue. The efficiency of the anti-adhesion effect was supported by the gross view (Figure 7) and by histological assessments (Figure 8). Furthermore, it is a synergistic effect of both the prevention of adhesion formation and promotion of tendon healing due to the respective function of each layer. The novel inner HA-loaded PCL layer of this biomimetic sheath was shown to be able to mimic the biological function of native tendon sheath, secreting HA to promote tendon healing and lubricate tendon gliding. According to the in vitro results of our study, better gliding and tendon healing can be achieved with more HA incorporated in the inner layer of sheath membrane. Furthermore, the mechanical properties of the bi-layer PCL-HA8% and 12% membranes were not significantly different. Thereafter, the bi-layer sheath membrane with inner PCL layer containing 12% HA was used for the in vivo test. Based on our successful results of the controlled release of HA, these functions are supported both by macroscopic and histologic evaluation and by the ratio of work of flexion assay in this study (Figure 7 and Figure 9). Furthermore, intrinsic tendon healing can be promoted by diffusion of nutrients from outside of the sheath to the repair site through the sheath membranes.[19] However, the increase in the breaking force showed no significant difference. This may be due to the limited number of specimens.

Our novel cell-free biomimetic sheath is very suitable for the clinical reality of tendon injuries because there is no requirement for *in vitro* culture and expansion of sheath cells and

synoviocytes. Our study demonstrates the preliminary success of the biomimetic bi-layer sheath membrane in a three week *in vivo* study. This critical period is the time when tendon healing is achieved and rehabilitation exercises are begun in the clinic and thus 3 weeks is sufficient for a preliminary investigation of the roles that such a sheath plays[19,30]. Moreover, although restoration of sheath integrity is believed to preserve nutrition of the tendons, provide them with a smooth gliding surface for tendons, and decrease peritendinous adhesions[6,35], the repaired sheath may disappear after suturing and is associated with poor tendon healing [36]. Consequently, it provides a therapeutic chance that our sheath membrane may completely mimic the biological function and structure of the native sheath, especially under the condition of sheath loss after injury during that critical period. However, before further use in the clinic, it will be necessary to investigate the later effects on tendon healing after the complete degradation of the biomimetic sheath. This will be the goal of our future studies. Furthermore, the biomimetic bi-layer sheath membrane provides a therapeutic chance to prepare two layers with differing and even opposite functions to satisfy the respective needs of tendon and its surrounding tissues. This is another issue deserving further investigation.

V. Conclusions

A biomimetic bi-layer sheath membrane can be prepared by sequential and microgel electrospinning. Using this system, appropriate flexibility and the controlled release of HA from the biomimetic sheath can be achieved. Our *in vitro* and *in vivo* results show that the outer PCL layer can reproduce the anti-adhesive role of the outer fibrotic layer while the inner HA-loaded PCL layer can mimic the biological function of HA secretion to promote tendon healing and gliding. Taken together, our results demonstrate that such a biomimetic bi-layer sheath membrane can release HA sustainably and shows preliminary promise in promoting tendon gliding and preventing adhesion.

AUTHOR INFORMATION

Corresponding Author

* E-mail: fancunyi888@hotmail.com; wgcui80@hotmail.com.

Funding Sources

This work was supported by the National Natural Science Foundation of China (81101361, 51003058 and 81171477), the Nano-tech Foundation of Shanghai (11nm0503100 and 1052nm05300) and the Doctoral Innovation Fund of SJTU (BXJ201235).

Notes

The authors declare no competing financial interest.

ACKNOWLEDGMENT

We thank Shanghai 9th People's Hospital, Shanghai Key Laboratory of Tissue Engineering, National Tissue Engineering Center of China and Shanghai Key laboratory of orthopedics implant for technique supports of cell culture and biomechanical analysis. We also thank Dr. Tianyi Wu for assistance of picture preparation.

ASSOCIATED CONTENT

Supporting Information

The tensile test results of PCL, PCL/HA single-layer and PCL/HA bi-layer membranes, the gross observation of electrospun PCL/HA solution, and the histological sections before and after trypsinization. This material is available free of charge via the Internet at http://pubs.acs.org.

ABBREVIATIONS

HA hyaluronic acid; PCL Poly(ε-caprolactone); C3 C3H10T½cells; SEM scanning electron microscopy; WCA water contact angle; PBS phosphate buffered saline.

REFERENCES

(1) Deng, M.; Kumbar, S. G.; Nair, L. S.; Weikel, A. L.; Allcock, H. R.; Laurencin, C. T. *Adv Funct Mater* **2011,** *21*, 2641-2651.

(2) Kyomoto, M.; Moro, T.; Saiga, K.; Hashimoto, M.; Ito, H.; Kawaguchi, H.; Takatori, Y.; Ishihara, K. *Biomaterials* **2012,** *33*, 4451-4459.

(3) Zhang, X. Z.; Bogdanowicz, D.; Erisken, C.; Lee, N. M.;Lu, H. H. *J Shoulder Elb Surg* **2012,** *21*, 266-277.

(4) Olszta, M. J.; Cheng, X. G.; Jee, S. S.; Kumar, R.; Kim, Y. Y.; Kaufman, M. J. Mat Sci Eng R **2007,** *58*, 77-116.

(5) William W. Peterson; P. R. M.; Janet Dunlap; Daniel S. Horwitz; Bary Kahn. *J Hand Surg* **1990,** *15*, 48-56.

(6) Gelberman R. H; V. B. J., Lundborg G. N, Akeson W. H. *J Bone Joint Surg* **1983,** *65*, 70-80.

(7) Uchiyama, S.; Amadio, P. C.; Coert, J. H.; Berglund, L. J.; An, K. N. *J Bone Joint Surg Am* **1997,** *79A*, 219-224.

(8) L. Hagberg, D. H.; K. Ohlsson. *J Hand Surg Br* **1992,** *17*, 167-171.

(9) Blewis, M. E.; Nugent-Derfus, G. E.; Schmidt, T. A.; Schumacher, B. L.; Sah, R. L. *Eur Cells Mater* **2007,** *13*, 26-38.

(10) Ozturk, A. M.; Yam, A.; Chin, S. I.; Heong, T. S.; Helvacioglu, F.; Tan, A. *J Biomed Mater Res A* **2008,** *84A*, 1120-1126.

(11) Xu, L.; Cao, D. J.; Liu, W.; Zhou, G. D.; Zhang, W. J.; Cao, Y. L. *Biomaterials* **2010,** *31*, 3894-3902.

(12) Mukai, T.; Kamitani, S.; Shimizu, T.; Fujino, M.; Tsutamoto, Y.; Endo, Y.; Hanasawa, K.; Tani, T. *Eur Surg Res* **2011,** *47*, 248-253.

(13) Hong, J.H.; Choe, J.W.; Kwon, G.Y.; Cho, D.Y.; Sohn, D.S.; Kim, S.W.; Woo, Y.C.; Lee, C.J.; Kang, H. *J Surg Res* **2011,** 166, 206-213.

(14) Liu, Y.; Skardal, A.; Shu, X.Z.; Prestwich, G.D. *J Orthop Res* **2008,** *26,* 562-569.

(15) Lee, J. H.; Go, A. K.; Oh, S. H.; Lee, K. E.; Yuk, S. H. *Biomaterials* **2005,** *26*, 671-678.

(16) Lo, H.Y.; Kuo, H.T.; Huang, Y.Y. *Artif Organs* **2010,** *34*, 648-653.

(17) Jing, Z.; Xu, X. Y.; Chen, X. S.; Liang, Q. Z.; Bian, X. C.; Yang, L. X.; Jing, X. B. *J Control Release* **2003,** *92*, 227-231.

(18) Verreck, G.; Chun, I.; Rosenblatt, J.; Peeters, J.; Van Dijck, A.; Mensch, J.; Noppe, M.; Brewster, M. E. *J Control Release* **2003,** *92*, 349-360.

(19) Bhavsar, D.; Shettko, D.; Tenenhaus, M. *J Surg Res* **2010,** *159*, 765-771.

(20) Jo, E.; Lee, S.; Kim, K.T.; Won, Y.S.; Kim, H.; Cho, E.C.; Jeong, U. *Adv Mater* **2009,** *21,* 968-972.

(21) Diaz, J.E.; Barrero, A.; Marquez, M.; Fernandez-Nieves, A.; Loscertales, I.G. *Macromol Rapid Commun* **2010,** *31,* 183-189.

(22) Piperno, S.; Gheber L.A.; Canton, P.; Pich, A.; Dvorakov, G.; Biffis, A. *Polymer* **2009,** *50,* 6193-6197.

(23) Cui, W. G.; Li, X. H.; Zhu, X. L.; Yu, G.; Zhou, S. B.; Weng. *Biomacromolecules* **2006,** *7*, 1623-1629.

(24) Cui, W. G.; Cheng, L. Y.; Li, H. Y.; Zhou, Y.; Zhang, Y. G.; Chang, J. *Polymer* **2012,** *53*, 2298-2305.

(25) Cui, W. G.; Li, X. H.; Zhou, S. B.; Weng, J. *J Appl Polym Sci* **2007,** *103*, 3105-3112.

(26) Haserodt, S.; Aytekin, M.; Dweik, R.A. *Glycobiology* **2011,** *21*, 175-183.

(27) Takeia, Y.G.; Honmaa, T.; Itoa, A. *J Immunoass and Immunoch* **2007,** *23*, 85-94.

(28) Ali M.; Byrne, M.E. *Pharm Res* **2009,** 26, 714-726.

(29) Cashman, J.; Burt, H. M.; Springate, C.; Gleave, J.; Jackson, J. K. Inflamm Res **2004,** *53*, 355-362.

(30) Ishiyama, N.; Moro, T.; Ishihara, K.; Ohe, T.; Miura, T.; Konno, T.; Ohyama, T.; Kimura, M.; Kyomoto, M.; Nakamura, K.; Kawaguchi, H. *Biomaterials* **2010,** *31*, 4009-4016.

(31) Gudemez, E.; Eksioglu, F.; Korkusuz, P.; Asan, E.; Gursel, I.; Hasirci, V. *J Hand Surg Am* **2002,** *27A*, 293-306.

(32) Jin Bo Tang, D. S., Qi G. Zhang. *J Hand Surg Am* **1994,** *21*, 900-908.

(33) Oh, S. H.; Kim, J. K.; Song, K. S.; Noh, S. M.; Ghil, S. H.; Yuk, S. H.; Lee, J. H. *J Biomed Mater Res A* **2005,** *72A*, 306-316.

(34) McCombe, D.; Kubicki, M.; Witschi, C.; Williams, J.; Thompson, E. W. *Clin Orthop Relat*

R **2006**, *451*, 251-256.

(35) Paul R; Manske, P. A. L. *J Surg Res* **1983,** *34*, 83-93.

(36) Jin-bo Tang, S. I. *J Hand Surg* **1994,** *19*, 636-640.

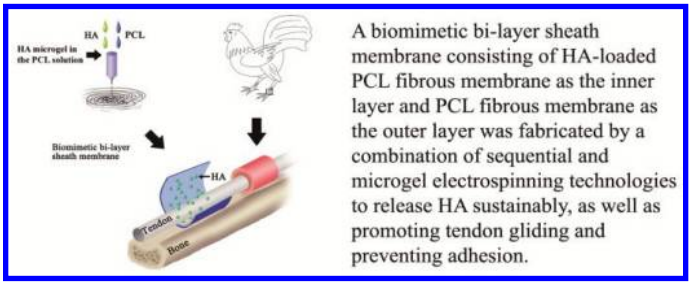

A biomimetic bi-layer sheath membrane consisting of HA-loaded PCL fibrous membrane as the inner layer and PCL fibrous membrane as the outer layer was fabricated by a combination of sequential and microgel electrospinning technologies to release HA sustainably, as well as promoting tendon gliding and preventing adhesion.

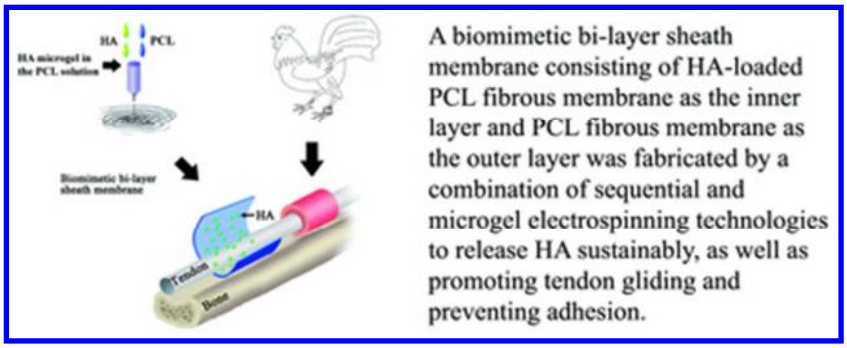

Biomimetic sheath membrane via electrospinning for anti-adhesion of repaired tendon
Shen Liu, Jingwen Zhao, Hongjiang Ruan, Tingting Tang, Guangwang Liu, Degang Yu, Wenguo Cui, Cunyi Fan

34x13mm (300 x 300 DPI)